Acta Biomed 2023; Vol. 94, N. 2: e2023141 DOI: 10.23750/abm.v94i2.14442

Original article

Crocin lessens desipramine-induced phospholipidosis biomarker levels via targeting oxidative stress- related PI3K/Akt/mTOR signaling pathways in the rat liver

Amal Ahmed El-Sheikh[1], Heba A. Mahmoud[2], Eman Ali El-Kordy[3,4], Amal M. Abdelsattar[5], Fatma H. Rizk[6], Radwa Mahmoud El-Sharaby[7], Shaimaa S. Mashal[8], Amira A. EL Saadany[2], Rania H. Shalaby[2,9], Amira M. Elshamy[10], Omnia Safwat El-deeb[10], Rowida Raafat Ibrahim[10], Hoda A. Ibrahim[10]

[1]Department of Anatomy, College of Medicine, Imam Abdulrahman Bin Faisal University, Dammam (Saudi Arabia); [2]Pharmacology Department, Faculty of Medicine, Tanta University, Tanta (Egypt); [3]Anatomy Department, College of Medicine, Imam Mohammad Ibn Saud Islamic University, Riyadh (Saudi Arabia); [4]Histology Department, Faculty of Medicine, Tanta University, Tanta (Egypt); [5]Anatomy Department, Faculty of Medicine, Tanta University, Tanta(Egypt); [6]Physiology Department, Faculty of Medicine, Tanta University, Tanta (Egypt); [7]Clinical pathology Department, Faculty of Medicine, Tanta University, Tanta (Egypt); [8]Internal Medicine Department, Faculty of Medicine, Tanta University, Tanta (Egypt); [9]Biomedical Sciences Department, Dubai Medical College for Girls, Dubai (UAE); [10]MedicalBiochemistry & Molecular Biology Department, Faculty of Medicine, Tanta University, Tanta(Egypt)

Abstract. *Background and aim:* Crocin is a pharmacologically active chemical found in the spice saffron from Crocus sativus L. It possesses antioxidant and anti-radical properties that can minimize the hepatic phospholipidosis triggered using the tricyclic antidepressant desipramine. The aim of this study was to examine the effect of crocin on desipramine-induced hepatic phospholipidosis targeting the oxidative stress-related PI3K/Akt/mTOR signaling pathways. *Methods:* Forty adult male rats were divided into 4 groups (n =10): control group, a group receiving intraperitoneal (IP) crocin (50 mg/kg/day), a group receiving IP desipramine (10 mg/kg/day), and a group receiving both IP crocin and desipramine. *Results:* After 3 weeks of treatment, the combined treatment group showed diminished desipramine-induced hepatic phospholipidosis, along with significant reductions in total oxidant status (TOS), the levels of inflammatory markers including interleukin 6 (IL6) and tumor necrosis factor α (TNF-α) and apoptotic markers including caspase3 and Bcl2 (B-cell lymphoma 2) while other markers including total antioxidant capacity (TAC), superoxide dismutase (SOD), phosphoinositide 3-kinases (PI3K), and mammalian target of rapamycin (mTOR) were increased. The gene expression of lysosomal enzymes including ELOVL6, SCD1 and HMGR was notably downregulated, while AP1S1 was upregulated in the combined treatment group compared to the desipramine group. No ultrastructural signs of hepatic phospholipidosis, in the form of multilamellar bodies, were apparent in the combined treatment group. *Conclusions*: These data collectively suggest that crocin has a protective effect against desipramine-induced phospholipidosis. (www.actabiomedica.it)

Key words: Phospholipidosis, desipramine, crocin, oxidative stress, apoptosis

Introduction

The pathogenesis of drug-induced hepatic injury is caused by direct effects of the drug molecule or its metabolites on cell biochemistry or by the triggering of an immunological response (1). Exposure to cationic amphiphilic drugs (CADs) promotes the buildup of intracellular phospholipids, which is a hallmark of drug-induced phospholipidosis (DIPLosis) (2). Among the CADs, tricyclic antidepressants (TCAs)

are known to cause this type of lipid storage illness (3). TCAs, such as desipramine, are used in treating obsessive-compulsive disorders, neuropathic pain, and enuresis, as well as attention deficit disorders. However, patients receiving these kinds of treatments frequently take these medications for long periods and therefore face serious risks of unanticipated adverse effects of long-term TCA usage (4). A diversity of side effects may arise during treatment with TCA, with the most serious complications involving the liver (5).

Studies have documented that, before reaching their target cells, TCAs pass through lipid membrane barriers. Consequently, the associations between these drugs, phospholipids, and lipid-containing membranes seriously affect their pharmacokinetics (6). The selective interchange of membrane proteins, lipids, and luminal components between organelles, by both endocytosis and exocytosis, depends on specific vesicular membrane proteins, which are exposed to the cytosolic side. The signals regulated by the cytoplasmic sides of membrane proteins are controlled by adaptor protein complexes (AP1-4), which are heterotetrameric coat protein complexes that also aid in gathering membrane lipids, organizing constituents of the vesicle fusion mechanism, and collecting supplementary constituents of the vesicle formation apparatus (7-9).

Cellular membrane physiology and signaling is controlled in part by an enzyme known as Stearoyl-CoA desaturase 1 (SCD1), which is responsible for producing monounsaturated fatty acids (from their corresponding saturated fatty acid precursors) and thereby broadly affects human physiology. Considering its principal role in lipid metabolism and body weight control, SCD1 has been recognized lately as a potential strategic goal for treating numerous diseases, such as nonalcoholic steatohepatitis and cancer, as well as skin diseases (10).

The fatty acid elongation cycle in mammals is regulated by elongation of very long-chain fatty acids proteins (ELOVL6), a family of enzymes that catalyze the first and rate-limiting condensation reaction of this cycle. At present, seven different ELOVL proteins (i.e., ELOVL1-7) are known to act specifically on saturated fatty acids (SFA) and monounsaturated fatty acids (MUFA). However, ELOVL 2, 4, and 5 can also act on polyunsaturated fatty acids (PUFA) (11). ELOVL 6 gene expression has been documented in the livers of mice overexpressing sterol regulatory element binding transcription factors that modulate the expression of multiple key lipogenic genes involved in the fatty acid metabolic pathway (12, 13). Similarly, the lysosome plays a cardinal role in lipid sorting, serving as a metabolic command and control center. It transmits diverse nutrient signals to mechanistic target of rapamycin complex 1 (mTorc1) kinase, which is a chief growth regulator. The function of mTorc1 is to promote anabolic processes, such as de novo lipogenesis, while suppressing lipid catabolism (14).

Recent studies have shown that lipid-related diseases can respond to treatments with substances that occur naturally in plants. One such substance is crocin, a pharmacologically active compound derived from Crocus sativus L., the source of the spice known as saffron that comprise many chemical substances, such as carbohydrates, minerals, vitamins, and pigments including crocin. which has confirmed antioxidant, anticancer, and radical scavenging properties (15), and recent studies have shown therapeutic effects of crocin for the treatment of hepatic fibrosis, steatosis, and diabetes-induced liver injury (16). To the best of our knowledge there is no studies discussed the effect of crocin on PI3K/Akt/mTOR signaling pathways in a model of desipramine induced-phospholipidosis and censored its effects through monitoring the levels of adaptor protein complex, stearoyl-co A desaturase and elongation of very long chain fatty acids protein and connected these networks of integrated biomarkers to oxidative stress-related phosphatidylinositol-3-kinase/ Akt/ mammalian target of rapamycin (PI3K/Akt/ mTOR) signaling pathways. So, the aim of the present study was to assess the protective effect of crocin against desipramine-induced hepatic insult in Wistar albino rats, with the overall goal of determining the mechanism by which crocin controls desipramine-induced liver phospholipidosis targeting oxidative stress–related PI3K/Akt/mTOR signaling pathways.

Material and methods

Study animals

The study carried out using forty adults male Wistar albino rats, with an average weight 150-230 g, from Tanta University Animal House. Rats were

housed in wire mesh cages at 20 ± 2 °C, with a relative humidity of 65 ± 10%, exposed to a 12-hour light/dark cycle, fed a standard laboratory diet and water and allowed to acclimatize one week before the experiment. National Institutes of Health's standards for the care and use of laboratory animals (NHI Publications No. 8023, revised 1996) were obeyed during carrying out all experimental work procedures to minimized animal suffering and were approved by the Ethical Committee of Medical Research, Faculty of Medicine, Tanta University (35334/3/22) with a date of release of permission 10/3/2022.

All animals received human care and that study protocol complied with the institutions guidelines and were conform to the Animal Research Reporting on in Vivo Experiments (ARRIVE).

Experimental design

Rats were indiscriminately equally assigned to four groups, each with ten rats; Group I served as control group: administered 0.5 ml saline intraperitoneally (I.P). Group II (crocin group): administered 50 mg/kg crocin I.P once a day for 3 weeks (17). Group III (Desipramine group) that was received desipramine 10 mg/kg IP once daily for 3 weeks (18). Group IV (desipramine & crocin group): concomitantly administered the same dose of crocin with desipramine intraperitoneally once a day for 3 weeks as described in Group II and Group III respectively. Unless otherwise mentioned, all reagents used throughout the study were of high analytical quality and obtained from Sigma/Aldrich USA. Desipramine hydrochloride ≥ 98% (TLC) powder (CAS number 58-28-6) was dissolved in saline. Crocin ($C_{44}H_{64}O_{24}$) powder 98% purity (CAS number 42553-65-1) was dissolved in saline.

Blood and tissue sample collection

Blood sampling: At the end point of the experiment, all animals were fasted overnight, anesthetized with Isoflurane 5% and euthanized to collect blood samples rapidly in sterilized tubes, allowed to clot by standing for thirty minutes at room temperature, and followed by twenty minutes centrifugation (1000 xg 4°C). Sera were gathered and preserved at -80°C for further biochemical investigation.

Hepatic tissue sampling: The liver was excised; one part was preserved in 2.5% glutaraldehyde for ultrastructural examination. The second part perfused in situ with ice□cold 0.9% (w/v) sodium chloride solution. Then, it was allowed to dry by blotting with filter paper and separated into two parts. One part was stored at –80°C till used for RNA extraction. The second part was used for preparation of tissue homogenate.

Preparation of hepatic tissue homogenate: At 4°C, one piece of each specimen was weighed and homogenized five times (w/v) in 0.1 M phosphate buffer using a Potter–Elvenhjem tissue homogenizer (pH 7.4). Homogenates were centrifuged at 70000 × g at 4°C for five minutes to eliminate cellular debris, and the resulting supernatant was then divided into aliquots and stored at –80°C till used for further analysis. Bradford technique was used to decide the protein concentration of rat liver homogenate (19).

Biochemistry measurements

Biochemical analysis: Serum was used for spectrophotometric determination of liver enzymes: aspartate transaminase [AST], alanine aminotransferase [ALT], alkaline phosphatase [ALP] and total bilirubin by using commercially available kits (Biodiagnostic, Giza, Egypt).

Analyzing of hepatic tissue phospholipids: Hepatic tissue homogenate total phospholipids were assayed using commercial kit (Sigma-Aldrich Chemie GmbH, Cat NO. MAK122) depending on the principle that different phospholipid such as lecithin, lysolecithin and sphingomyelin were hydrolyzed enzymatically to choline which was determined using choline oxidase and a H_2O_2-specific dye at 570 nm. Rat lipoprotein-associated phospholipase A2 (LPLA2) was also assessed (MyBiosource, Inc. Southern California, San Diego (USA) Catalog No: MBS704213).

Assay of hepatic tissue oxidative stress and inflammatory biomarkers: Both hepatic total oxidant status (TOS) and total antioxidant capacity (TAS) levels were assayed colorimetrically according to Erel's method (20, 21). TOS assay was based on the principle that samples' oxidants convert ferrous ion to ferric ions which by its turn forms a colored complex with the chromogenic reagent. This complex was measured spectrophotometrically at 560 nm directly

proportional to the amount of oxidant in the sample. Standard 20 μmol/L H_2O_2 solution was used. Results were stated in μmol H_2O_2 Equiv/L (20). TAS assay was based on the standard that the colored radical is decolorized depending on the antioxidant molecules total concentrations which diminish the colored ABTS (2,2'-azino-bis (3-ethylbenzothiazoline-6-sulfonic acid) radicals in the sample. Trolox was used as standard calibrator. Finally, all results were conveyed as mmol Trolox Equivalent/L (21).

Superoxide dismutase (SOD) enzyme activity was measured by using commercially available kits (Biodiagnostic, Giza, Egypt). Tumor necrosis factor α (TNF□α) level was assayed using commercial supplied kits (Chongqing Biospes company, China. catalog number: BEK1214). Interleukin 6 (IL-6) level was assayed using commercial supplied kits (Abcam company, USA. Catalog number: (ab100772). All ELISA techniques were done according to the manufacturer's commands using ELISA Reader (Stat Fax®2100, Fisher Bioblock Scientific, France), at 450nm wavelength.

Assay of hepatic tissue PI3K, mTOR, and apoptotic biomarkers B-cell lymphoma 2 (Bcl2) and caspase 3: PI3K, mTOR, Bcl2 and caspase 3 hepatic tissue homogenate levels were estimated using an enzyme-linked immunosorbent assay (ELISA) with available commercial kits (MyBiosource, Inc. Southern California, San Diego (USA) Catalog No: MBS726795, MBS8808126, MBS2515143 and MBS2088703, respectively) according to manufacturer guidelines.

Quantitative measurement of AP1S1, ELOVL6, SCD1 and HMGR gene mRNA expression by quantitative real□time reverse transcription polymerase chain reaction (RT□PCR)

RNA extraction and Purification and cDNA synthesis: Total RNA was extracted from hepatic tissues using a Gene JET RNA Purification Kit (Thermo Fisher Scientific, Waltham, MA, # K0731) according to the manufacturer's protocol. Total RNA concentration and purity were determined by assessing OD260 and OD260/280 ratio, respectively, on a NanoDrop spectrophotometer (NanoDrop Technologies, Inc. Wilmington). RevertAid H Minus Reverse Transcriptase was used to reverse transcribe total RNA samples (5μg) to produce cDNA for PCR that was stored at -80 ° C.

Real-time quantitative PCR: The cDNA was used as a template to determine relative expression of AP1S1, ELOVL 6, SCD1 and HMGR genes by usage of StepOnePlus real-time PCR system (Applied Biosystem, USA) according to manufacturer's instructions. By Primer 5.0 software, primers were designed as follow: AP1S1 F: 5' - GCCATCGAGGGCCAAGA -3', and R: 5'- TTTGTCTAAGAGCTCCACGTATCG-3'. ELOVL6 F: 5'- GCTACAACGGAGCAGAGGAC -3', and R: 5'- CCATTTTCAAGCCAACCAGT -3'. SCD1 F: 5' - CTGTTAGCCCAGCCTCACTC -3', and R: 5'- GTCTGCAGGAAAACCTCTGC -3'. HMGR F: 5' -CTT GAC GCT CTG GTG GAA TG-3', and R: 5'- AGT TGG AAG CAC GGA CATA-3'. The housekeeping gene β-actin primer sequences F: 5'-AGCCATGTACGTAGCCATCC-3' and R:5' AGCCATGTACGTAGCCATCC -3' was used as a reference for fold change in target gene expression calculation. The threshold cycle (Ct) $2^{-}\Delta\Delta^{Ct}$ method (22) was used to investigate the relative expression level of genes standardized to GAPDH.

Hepatic tissue processing for transmission electron microscopy: Small pieces from liver tissue (1 mm maximum) were fixed in 2.5% glutaraldehyde in 0.1 M Sorenson's buffer, washed overnight in 0.1M Sorenson's buffer, post-fixed in buffered 1% osmium tetroxide for 45 min, dehydrated in ethanol, infiltrated in propylene oxide and resin, and impregnated in medium epoxy resin. Sections were sectioned with ultramicrotome, dissected ultrathin, placed on copper grids, and stained with uranyl acetate and lead citrate (23). All electron micrographs were taken by a JEOL JEM 100 SX transmission electron microscope (Tokyo, Japan) at 80kv in the Electron Microscopic Unit, Faculty of Medicine, Tanta University, Egypt.

Statistical analysis

Statistical tests were performed using the SPSS software program (IBM SPSS Statistics for Windows, IBM Corp, version 23.0. Armonk, NY, USA). The results were expressed as mean ± standard deviation (SD). Statistical comparisons between different groups were conducted using the one-way analysis of variance (ANOVA) test followed by LSD post-hoc test for multiple comparisons. Statistical significance was considered when p values <0.05.

Results

Effect of desipramine and crocin on body, liver weight, and liver function tests

The rat initial body weight did not show any significant changes among the study groups. By the end of the experiment, the final body and liver weights were significantly higher for the desipramine group than for the control and crocin groups. The combined administration of crocin and desipramine significantly prevented much of the increase in the final body and liver weights observed in the desipramine group. Crocin administration alone did not cause significant changes in liver or body weights compared with the control group (Table 1).

Desipramine treatment impaired the liver function, as indicated by the significantly higher serum ALT, AST, ALP, and bilirubin levels in the desipramine group than in the control group. The combined administration of crocin and desipramine resulted in significantly improved liver function, as evidenced by the significantly lower values for the liver function tests than were determined in the desipramine group. Rats administered crocin alone showed similar liver function test results to those of the untreated control group (Table 1).

Effect of desipramine and crocin on hepatic phospholipidosis biomarkers

The hepatic total phospholipid level was significantly higher and the hepatic LPLA2 level was significantly lower in the desipramine group than in the untreated control group. By contrast, the hepatic total phospholipid level was significantly lower and the hepatic LPLA2 level was significantly higher in the combined treatment group than in the desipramine group. Rats treated with crocin treatment showed similar levels of these biomarkers to those of the untreated controls (Table 2).

Effect of desipramine and crocin on hepatic oxidative stress and inflammatory biomarkers

The hepatic tissue homogenate levels of TOS, IL6 and TNF-α were significantly higher while the TAC and SOD levels were significantly lower, in the

Table 1. Effect of desipramine and crocin on body weight, liver weight and liver function tests.

	Control group	Crocin group	Desipramine group	Desipramine +crocin group
Initial body weight (g)	165.60±6.75	167.70±4.55	166.00 ±6.16	163.70 ±7.06
Final body weight (g)	217.50±8.317	219.00±6.62	292.30±4.42 [a,b]	238.20±6.03 [a,b,c]
Liver weight (g)	4.39 ± 0.18	4.40 ± 0.31	6.84 ± 0.33 [a,b]	5.46 ± 0.30 [a,b,c]
ALT (U/L)	48.50 ± 5.50	46.50 ± 5.93	166.10 ±7.03 [a,b]	94.00 ± 6.50 [a,b,c]
AST(U/L)	88.70 ± 6.88	89.10 ± 6.90	197.30 ±9.43 [a,b]	157.70 ± 5.74 [a,b,c]
ALP (U/L)	204.30 ±10.33	202.50±10.62	428.90 ±13.69 [a,b]	330.20 ±9.10 [a,b,c]
Bilirubin (mg/dl)	0.32 ± 0.071	0.38 ± 0.04	2.22 ± 0.08 [a,b]	1.47 ± 0.15 [a,b,c]

Note: Data are expressed as mean ± SD. [a]p<0.05 vs control group, [b]p<0.05 vs crocin group and [c]p<0.05 vs desipramine group.

Table 2. Effect of desipramine and crocin on the phospholipidosis assay.

	Control group	Crocin group	Desipramine group	Desipramine +crocin group
Total phospholipids (mg/mg.tissue homogenate)	88.70 ± 2.50	88.20 ± 3.01	148.67 ± 3.35 [a,b]	117.57 ± 2.61 [a,b,c]
LPLA2 (ng/ mg.tissue.ptn)	148.20 ± 4.29	149.40 ± 5.97	54.50 ± 6.29 [a,b]	97.50 ± 5.82 [a,b,c]

Note: Data are expressed as mean ± SD. ap<0.05 vs control group, bp<0.05 vs crocin group and cp<0.05 vs desipramine group.

Table 3. Effect of desipramine and crocin on hepatic oxidative stress and inflammatory biomarkers.

	Control group	Crocin group	Desipramine group	Desipramine +crocin group
TOS (μmol. Equiv./ mg tissue protein)	13.54 ± 0.54	13.50 ± 0.44	20.41± 0.68 [a,b]	16.90 ± 0.44 [a,b,c]
TAC (mmol. Equiv./ mg tissue protein)	4.82 ± 0.09	4.78 ± 0.11	1.57 ± 0.13 [a,b]	3.65 ± 0.07 [a,b,c]
SOD (U/mg tissue protein)	217.10 ± 9.33	213.30 ± 5.83	115.20 ±6.37 [a,b]	166.20 ± 5.07 [a,b,c]
IL6 (pg/mg tissue protein)	37.90 ± 3.70	38.44 ± 4.45	140.24 ± 6.20[a,b]	72.84 ± 4.73[a,b,c]
TNFα (pg/mg tissue protein)	30.00 ± 5.08	29.98 ± 5.70	168.95 ± 3.71[a,b]	78.43 ±5.98[a,b,c]

Note: Data are expressed as mean ± SD. ap<0.05 vs control group, bp<0.05 vs crocin group and cp<0.05 vs desipramine group.

Table 4. Effect of desipramine and crocin on apoptosis biomarkers.

	Control group	Crocin group	Desipramine group	Desipramine +crocin group
PI3K (ng/ mg tissue protein)	0.92 ± 0.03	0.91±0.03	0.53 ± 0.04 [a,b]	0.74 ± 0.03 [a,b,c]
mTOR (ng/ mg tissue protein)	1.79 ± 0.04	1.86 ± 0.08	1.09 ± 0.11 [a,b]	1.35 ± 0.13 [a,b,c]
Caspase3 (ng/ mg tissue protein)	0.14 ± 0.02	0.15 ± 0.01	0.81 ± 0.03 [a,b]	0.61 ± 0.05 [a,b,c]
Bcl2 (ng/ mg tissue protein)	1.09 ± 0.16	1.06 ± 0.13	1.68 ± 0.04 [a,b]	1.49 ± 0.04 [a,b,c]

Note: Data are expressed as mean ± SD. ap<0.05 vs control group, bp<0.05 vs crocin group and cp<0.05 vs desipramine group.

desipramine group than in the control group. However, the group given the combined desipramine and crocin treatment showed a notable decline in the TOS, IL6 and TNFα levels and elevation in the TAC and SOD levels when compared with the desipramine group. The oxidative stress and inflammatory marker levels were similar in both the crocin-treated and control groups (Table 3).

Effect of desipramine and crocin on apoptosis markers

The caspase3 and Bcl2 levels were significantly higher, and the PI3K and mTOR levels were notably lower in hepatic tissue homogenates from the rats treated with desipramine than in the control group. By contrast, the caspase3 and Bcl2 levels were significantly lower and the PI3K and mTOR levels were significantly higher in the group given the combined treatment with crocin and desipramine than in the group treated with desipramine alone. Rats treated with crocin alone and the untreated control rats showed similar levels of these markers (Table 4).

Effect of desipramine and crocin on gene expression of lysosomal enzymes

Gene expression of ELOVL6, SCD1 and HMGR was significantly upregulated, and gene expression of AP1S1 was significantly downregulated in the desipramine treatment group compared with the untreated control group. By contrast, the combined administration of crocin and desipramine resulted in significant downregulation of ELOVL6, SCD1 and HMGR and significant upregulation of AP1S1 compared to the expression levels in the desipramine group. Crocin administration alone caused no significant changes in gene expression of lysosomal enzymes compared to the untreated control group (Figure 1).

Electron microscopy results

Histopathological evaluation of liver sections from the animals in the control and crocin groups revealed a normal histological appearance for both groups. Semithin sections of the control group liver revealed a normal liver lobular architecture, with polyhedral hepatocytes

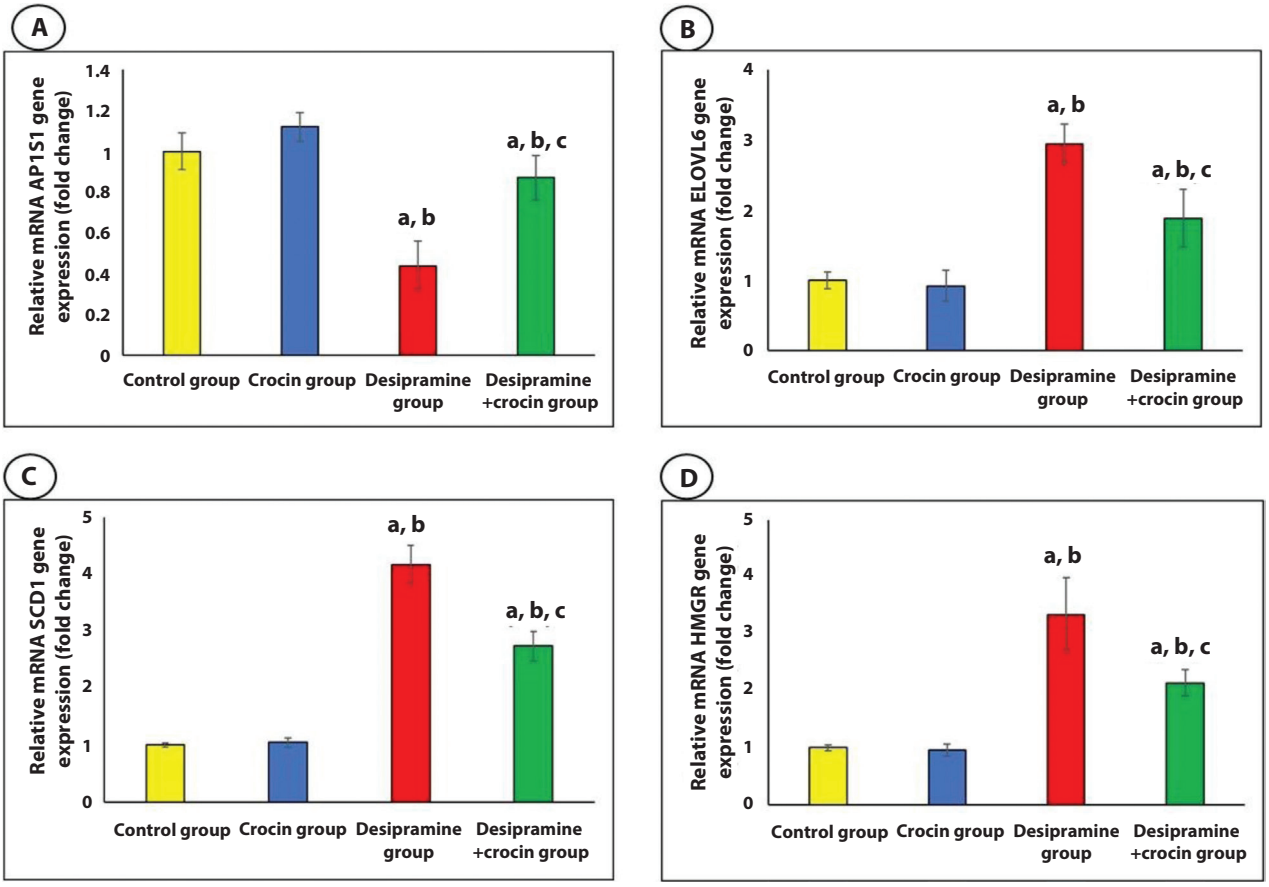

Figure 1. Effect of desipramine and crocin on gene expression of lysosomal enzymes. (A) Relative mRNA AP1S1 gene expression (fold change). (B) Relative mRNA Elovl6 gene expression (fold change). (C) Relative mRNA Scd1 gene expression (fold change). (D) Relative mRNA Hmgr gene expression (fold change). Data are expressed as mean ± SD. ap<0.05 vs control group, bp<0.05 vs crocin group and cp<0.05 vs Desipramine group.

arranged in irregular cords around the sinusoids. The hepatocyte nuclei were centrally placed and contained large distinct nucleoli (Figure 2A). Electron microscopy analysis of the hepatocytes revealed large, round, euchromatic nuclei and cytoplasm containing many organelles. The hepatic sinusoids were lined by Kupffer cells, and the space of Disse was occupied by numerous microvilli (Figure 2B). Bile canaliculi were formed by the cell membranes of neighboring hepatocytes and showed small microvilli and tight-junction complexes (Figure 2C).

The semithin sections from the desipramine-treated group showed marked alterations, including disturbance of the normal parenchymal architecture of the liver, disorganization of the hepatic cords, and narrowing of many sinusoids. Hepatocellular degeneration was evident, as indicated by cytoplasmic vacuolization and pyknotic nuclei, as well as variations in the nucleus size (Figure 3A). Electron microscopy analysis revealed massive alterations in hepatocyte morphology, as the cytoplasm of some cells became clear and completely disarrayed, with few dispersed organelles. The nuclei showed different shapes and sizes, with some appearing small, irregular, and electron dense and others showing peripheral condensation of heterochromatin. The rough endoplasmic reticulum became disaggregated, with its cisternae dispersed and altered in length in some cells (Figure 3B, C and D). The hepatocytes contained many lysosomes that were locally enriched in the peri-canalicular regions (Figure 4A). Unicentric

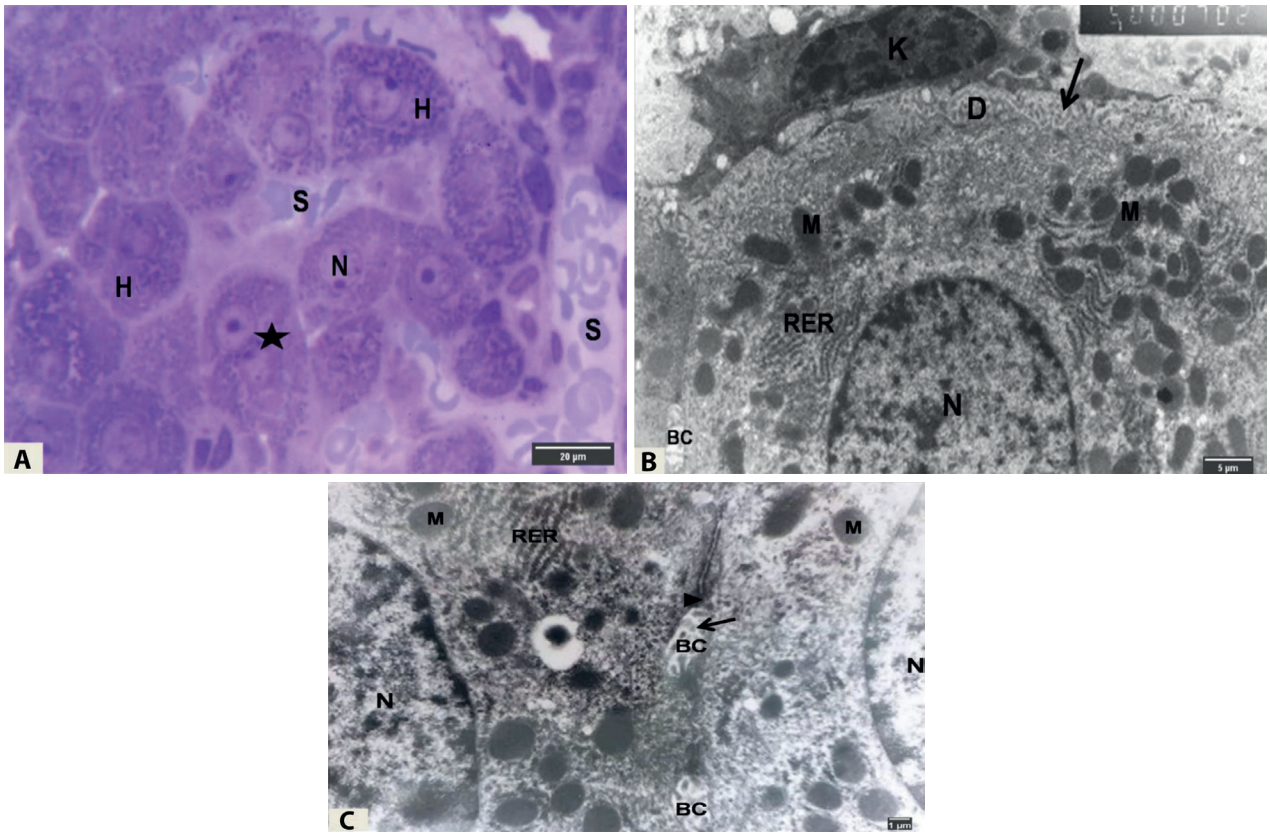

Figure 2. Semithin and ultrathin sections from control rat's liver showing a) normal hepatocytes (H) arranged in plates or cords between which are the blood sinusoids (S), the nuclei (N) are central with large prominent nucleoli. Star points to binucleated hepatocytes (Toluidine blue. original magnification×1000, scale bars: 20µm). b) One hepatocyte with spherical euchromatic nucleus (N), well organized rough endoplasmic reticulum (RER) and numerous mitochondria (M). K, Kupffer cell, D, space of Disse with numerous microvilli (→) and BC, bile canaliculus (original magnification×5000, scale bars: 5µm). c) Two adjacent hepatocytes with bile canaliculi (BC) between them. Note the microvilli (→) in its lumen and the junctional complexes (►). Mitochondria (M), rough endoplasmic reticulum (RER), nucleus (N) (original magnification×10000, scale bars: 1µm).

lamellated membranous inclusions were also seen in the cytoplasm of the vast majority of the hepatocytes (Figure 4D) and in the lumen of some bile canaliculi and cytoplasm of Kupffer cells (Figure 4C and D).

The semithin sections from the animals given the combination of desipramine and crocin showed nearly normal structures of the hepatocytes, with most containing granular cytoplasm and some with dense cytoplasm (Figure 5A). The ultrathin sections of this group showed that most of the hepatocytes had euchromatic nuclei with multiple large and prominent nucleoli, while the cytoplasm retained its normal appearance, with intact rough endoplasmic reticulum and mitochondria. However, a few hepatocytes showed mild vesiculation. (Figure 5B, C and D). No lamellated bodies were observed in the combined treatment group.

Discussion

Desipramine significantly increased hepatic tissue homogenate levels of total phospholipids, TOS, IL6, TNF-α, caspase3, Bcl2 and gene expression of ELOVL6, SCD1 and HMGR, while lowering LPLA2, TAC, SOD, PI3K, mTOR and AP1S1. Crocin and desipramine combined treatment decreased hepatic total phospholipids, TOS, IL6, TNF-α, caspase3, Bcl2 levels and gene expression of ELOVL6, SCD1

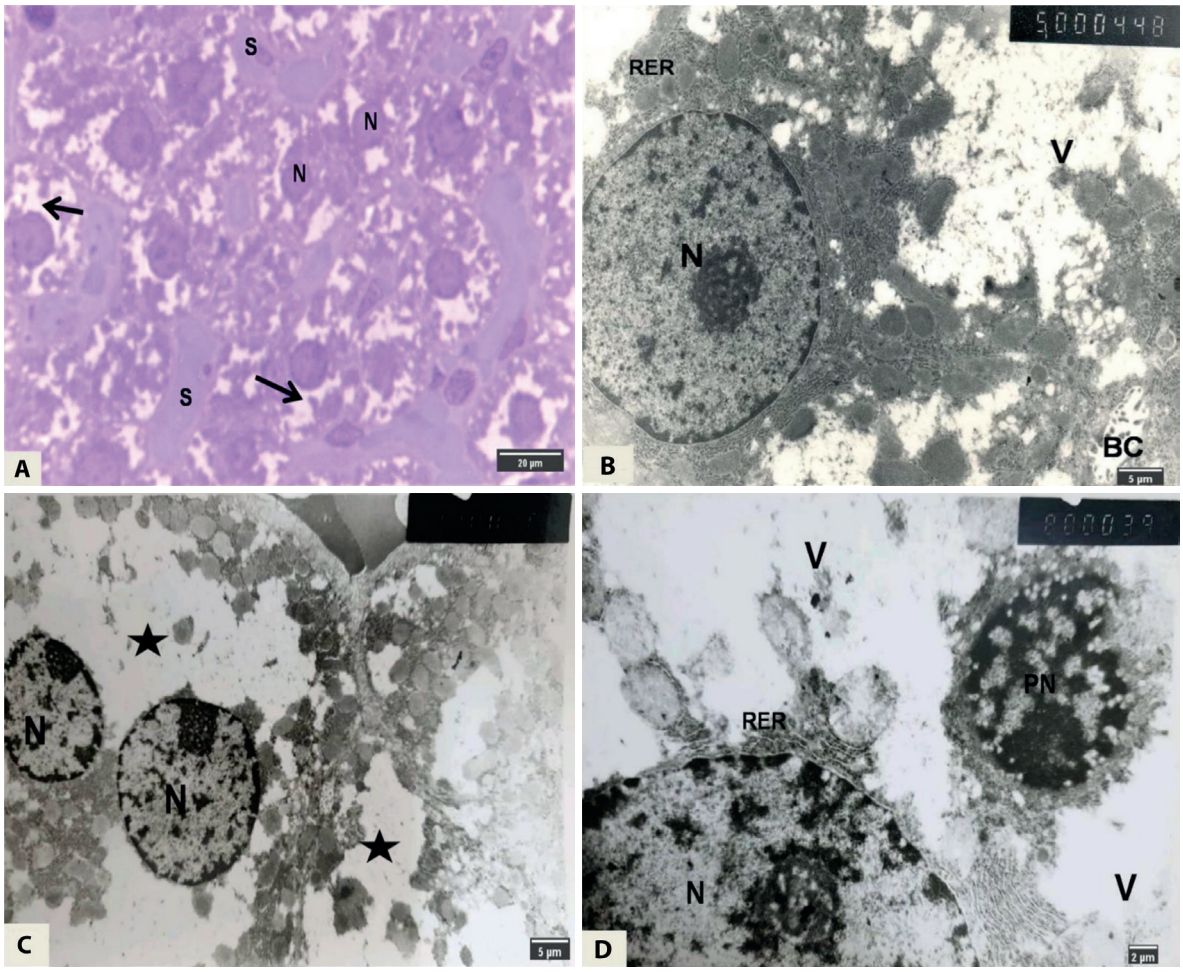

Figure 3. Semithin and ultrathin liver sections of group III showing a) loss of the normal parenchymal architecture of the liver. The hepatocytes appeared with abnormally dispersed cytoplasm (→) and pyknotic nuclei (N). Narrowing in blood sinusoids (S) was noticed (Toluidine blue. original magnification×1000, scale bars: 20µm). b) Hepatocyte with disorganization, vacuolation of the cytoplasm (V) and destructed endoplasmic reticulum (RER). Note the bile canaliculus with few microvilli (BC) and hepatocyte's nucleus (N) (original magnification×5000, scale bars: 5µm). c) Hepatocytes with clear completely disarrayed cytoplasm, containing few organelles (stars) and peripheral heterochromatic condensation of the nuclei (N) (original magnification×5000, scale bars: 5µm). d) Hepatocyte with small irregular electron dense nucleus (PN) and other nucleus appeared normal (N), severely vacuolated cytoplasm (V), destructed RER (original magnification×8000, scale bars: 2µm).

and HMGR, but improved liver function and histopathological changes. CADs cause intracellular lysosomal buildup of phospholipids, leading to DIPLosis (24). Indigestible drug-lipid complexes are formed by direct binding of CADs to lipids, resulting in sequestration of CADs in lysosomes (25). CADs bind to phospholipids to prevent degradation and lipid breakdown, promoting lipid biosynthesis (26). CAD desipramine provokes hepatic DIPLosis by increasing total phospholipids and decreasing LPLA2 levels (27-30).

Previous research has indicated that Cell proliferation and intracellular transport may be inhibited by an increase in intracellular phospholipids (31). The downregulation of genes like AP1S1, which is involved in lysosomal enzyme transport indicates an inhibition of the trafficking of newly generated lysosomal enzymes between both lysosomes and the trans-Golgi network (32).

Increases in phospholipid biosynthesis due to upregulation of genes such as ELOVL6 (33, 34) and

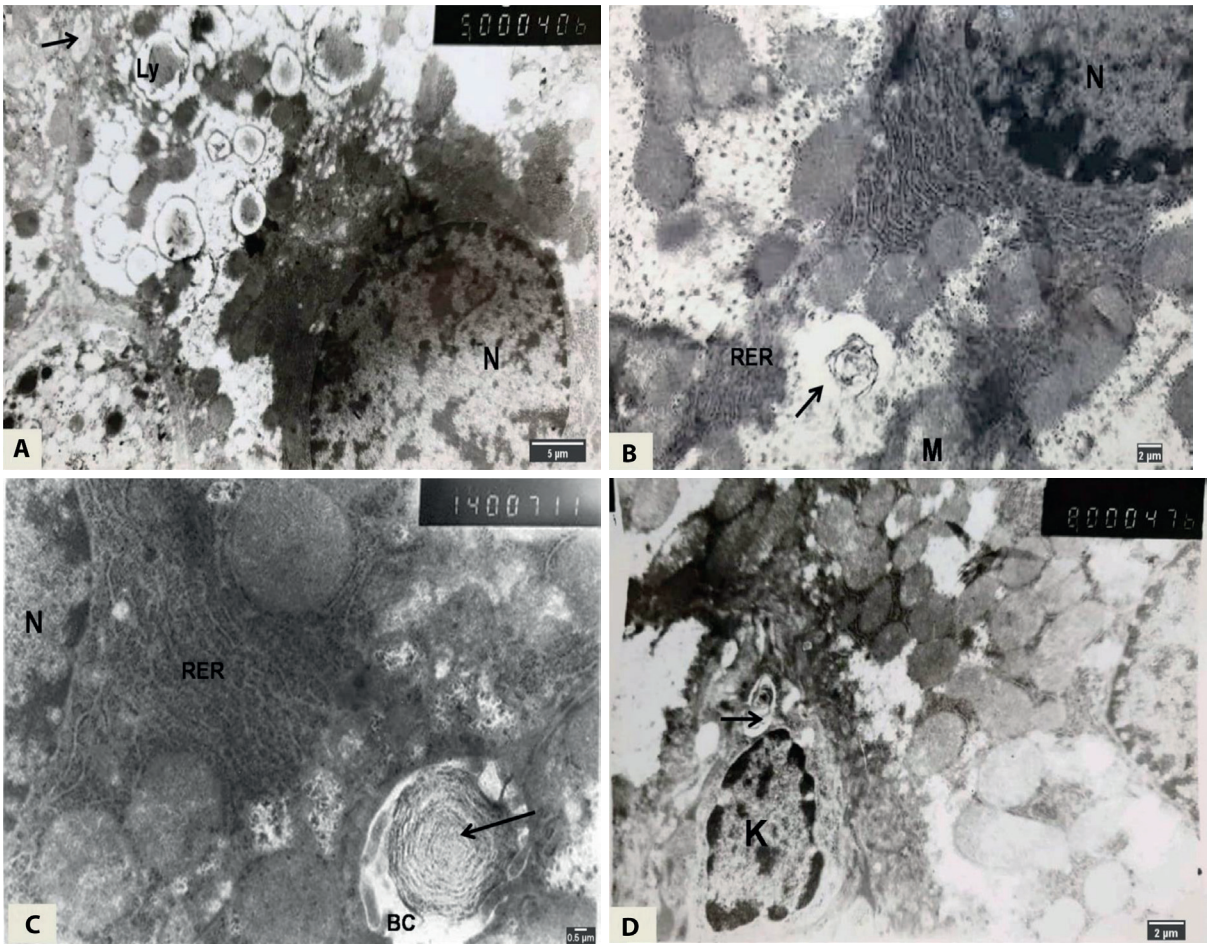

Figure 4. An electron micrograph of hepatocytes of group III rats showing a) severely destructed hepatocytes with numerous lysosomes (Ly) near the bile canaliculus (→). N, hepatocyte's nucleus (original magnification×5000, scale bars: 5µm). b) lamellated membranous bodies in the cytoplasm (→), destructed RER, mitochondria (M) and nucleus with peripheral heterochromatin condensation (N) (original magnification×8000, scale bars, 2µm). c) lamellated bodies (→) in bile canaliculus. Rough endoplasmic reticulum (RER), nucleus (N). (Original magnification×14000, scale bars, 0.5µm). d) Kupffer cells (K) showing lamellar body (→) in their cytoplasm (original magnification×8000, scale bars: 2 µm).

SCD1 (35), which are involved in fatty acid biosynthesis, promote cholesterol biosynthesis, as shown by the upregulation of cholesterol biosynthesis-related genes such as HMGR (36). HMGR is embedded in the endoplasmic reticulum membrane and elevates intracellular cholesterol, which then stimulates the unfolded protein response in macrophages (37). Enhanced biosynthesis of phospholipids and cholesterol and the resulting lipid overload, in addition to inhibition of lysosomal phospholipase activity and lysosomal enzyme transport, could directly trigger DIPLosis.

Desipramine is associated with hepatotoxicity and hepatic necrosis, with onset 2-3 weeks, with an increase in serum ALT, AST, ALP, and bilirubin levels (38, 39). The pathophysiological mechanism most often proposed to explain these results is idiosyncratic, dose-dependent, and unpredictable and is triggered either by immune-mediated liver injury or by direct cellular damage (40). Liver injury is caused by an accumulation of desipramine in lysosomes, leading to osmotic swelling and massive vacuolization in the cytoplasm (41, 42). Pyknotic and heterochromatin changes in nuclei are signs of cell death, explained by Trump et al. as early phase of irreversible injury (43). The presence of many lysosomes in the hepatocytes may also indicate a mechanism by which the liver

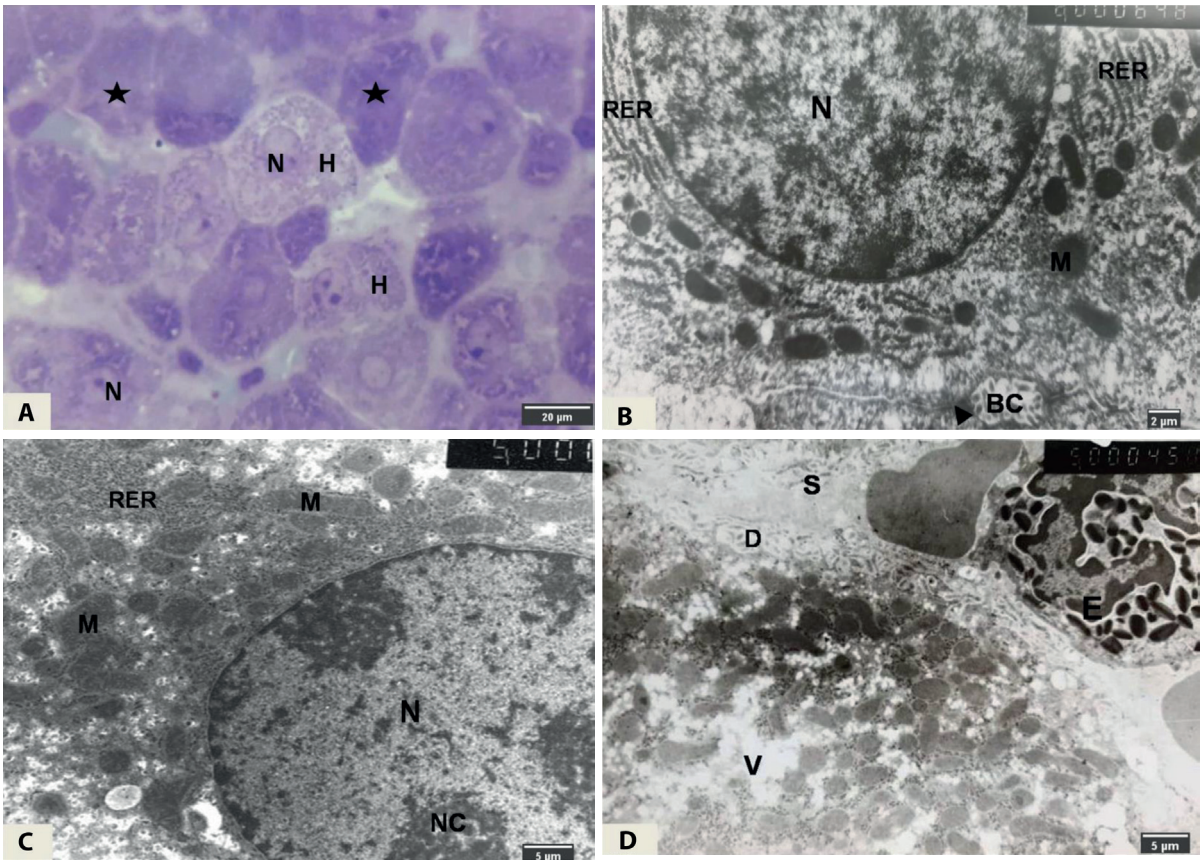

Figure 5. Semithin and ultrathin liver sections of group IV showing: a) most hepatocytes (H) have granular cytoplasm with vesicular nuclei (N) and few have dense cytoplasm (stars) (Toluidine blue ×1000). b) hepatocytes have euchromatic nuclei (N), Bile canaliculus (BC), tight junction (▶). Regularly arranged endoplasmic reticulum (RER), mitochondria (M) (×8000). c) hepatocytes have euchromatic nuclei (N) with large multiple nucleoli (NC). Mitochondria (M), rough endoplasmic reticulum (RER) (×5000). d) hepatocyte with mild vesiculation of cytoplasm (V). Space of Disse (D), eosinophil (E) at blood sinusoid (S) (×5000).

eradicates or diminishes cell damage caused by desipramine by lysosome triggering (44). The Kupffer cells also share in the removal of lamellar bodies (45).

Desipramine treatment can markedly provoke oxidative stress by increasing the production of reactive oxygen species (ROS), decreasing antioxidant levels, and causing a subsequent oxidant/antioxidant imbalance that, in turn, disturbs cellular proliferation, alters metabolism, and promotes angiogenesis, ultimately leading to cell death (46). Our results demonstrated an elevated TOS with a concomitant decrease in both TOC and SOD enzyme levels in the hepatic tissues of the desipramine group. The levels of several inflammatory biomarkers, including IL6 and TNF-α, were also increased by desipramine administration. Both oxidative stress and inflammatory status promote the overproduction of ROS, which can induce mitochondria damage and loss of mitochondrial membrane potential and subsequent apoptosis cascades via the mitochondria-mediated cell death pathway (47, 48). Desipramine-induced apoptosis (49, 50) was also confirmed by our results showing elevated levels of the apoptotic biomarkers caspase 3 and Bcl2 and an associated decrease in the levels of both PI3K and mTOR in hepatic tissue homogenates of the desipramine-treated rats.

Desipramine treatment also caused a significant decrease in the phosphorylation of extracellular-signal-regulated kinase 1 and 2 (ERK1/2) - PI3K, c-Jun N-terminal kinase (JNK), and p38 mitogen-activated

protein kinases (MAPKs). So, desipramine-induced cell death can be moderated using MAPK inhibitors. The PI3K signaling pathway enhances cell survival and has been reported to participate in apoptosis in different tissues (51). Lipid second messengers, mainly those resulting from the polyphosphoinositide cycle, also play fundamental roles in several cell signaling networks, in addition to those that induce cell death, and these messengers are related to many lipid modifications. Those occurring at the cytoplasmic membrane may contribute to inhibition of the PI3K/Akt/mTOR signaling pathway, which is situated on the inner cytoplasmic membrane and modulates downstream signal transduction cascades that are involved in the regulation of metabolism, energy equilibrium, and cell death (52).

Crocin, the water-soluble carotenoid and the most important abundant compound of the saffron spice, has been reported to have several pharmacological activities (53), including antioxidant, anti-inflammatory (54), hypolipidemic, antidepressant, and memory and learning enhancement effects (55, 56). Interestingly, crocin administration reduced the increases in liver weight and markedly decreased the serum levels of AST and ALT in db/db mice, but its effects were inhibited by downregulation of 5' adenosine monophosphate-activated protein kinase (AMPK). Crocin also significantly reduced the high levels of liver triglycerides, and this effect was also inhibited by AMPK downregulation. These findings suggested that crocin moderated hepatic injury by activation of AMPK signaling. Some evidence indicates that crocin can decrease blood glucose levels and insulin resistance, improve lipid profiles, and protect against obesity (57) while also exerting a protective effect against beryllium chloride-induced oxidative damage of hepatic tissue (58). Crocin is also effective at preventing lipid peroxidation and significantly elevates the levels of antioxidant enzymes (SOD and GSH) in methamphetamine-induced neurotoxicity, and the antioxidant properties of crocin are suggested as a possible mechanism for its neuroprotective potential (59).

In the present study, desipramine treatment caused significant morphological alterations in the rat livers, but the addition of crocin significantly diminished these degenerative changes and reduced the extent of hepatic phospholipidosis, as no lamellar bodies were observed in hepatocytes or Kupffer cells in the livers of animals that received the combined treatment. This is consistent with the results observed by Salahshoor et al., who also found that crocin diminished liver damage caused by morphine toxicity and who proposed that crocin action might occur by augmentation of the antioxidant network in hepatocytes and increased protection against damaging free radicals (60). In the present study, the nuclei in the livers of rats administered the combined treatment showed large multiple nucleoli, which can be explained by a successive increase in nucleolus size due to increases in ribosomal-RNA and protein synthesis, suggesting regeneration and recovery of the hepatocytes (61).

Several studies have confirmed the protective role of crocin against deleterious oxidative stress-induced effects. Crocin has a protective effect against oxidative stress-mediated apoptosis in rat livers damaged by diazinon (62), in rat kidneys and skeletal muscles subjected to ischemia-reperfusion-induced oxidative damage, and in rat neuronal cells subjected to acrylamide-induced neurotoxicity (63). The evidence shows that the antioxidant capacity of crocin is the most essential driver of its protective effects. Importantly, crocin has significant health benefits that include suppression of oxidative stress (64), and antiapoptotic activities (65), as well as modulation of signal transduction (66).

The mechanism proposed to explain the improvement in liver ischemia-reperfusion injury by crocin is thought to involve mainly an elevation of antioxidant enzyme activities, improvement of serum levels of liver enzymes, and downregulation of miR-122 expression. Administration of bisphenol A (BPA), an endocrine-disrupting environmental pollutant chemical, significantly upregulated miR-122 expression, but this effect was significantly decreased by the addition of crocin, suggesting a novel mechanism for crocin protection against hepatic injury (66). One proposal is that a surplus of pro-oxidant species leads to MAPK activation, which then elicits a series of downstream events that participate in the development of different human diseases (67). Some evidence supports a role for miR-122 in maintaining lipid metabolism and liver homeostasis, as miR-122 inhibition has been used to decrease plasma cholesterol levels and liver triglyceride buildup,

as well as the expression of various genes implicated in the synthesis of fatty acids (e.g., fatty acid synthase, acetyl-CoA carboxylase, and SCD) (68).

Crocin administration also enhanced Phosphorylated Akt (P-Akt) levels and decreased apoptosis due to infrared damage in retinal cells via the PI3K/Akt signaling pathway. Of note, crocin administration suppressed degeneration-related inflammation and catabolism in rat intervertebral discs, possibly by suppression of JNK activation (69). Crocin lowered oxidative stress and the pro-inflammatory response of microglial cells in diabetic retinopathy by promoting PI3K/Akt signaling, but it did not alter p- Akt levels in the livers of BPA-exposed rats (70). The neuroprotective mechanism of crocin in Parkinson's (PD) apparently occurred through modulation of the PI3K/Akt/mTOR pathway and minimizing the activity of the major apoptotic players implicated in PD pathogenesis. These metabolic alterations were also reflected in improved motor function. Thus, using crocin to target signaling molecules, including miRNA-7, miRNA-221, p-PRAS40, and mTOR, might identify interesting targets for delaying the development of diseases ranging from PD to DIPLosis and potentially enabling future preventive treatments (71).

Limitations

Our results should be further validated by in vitro trials to provide further supporting data and to gain a greater mechanistic understanding of the ameliorating effect of crocetin in desipramine-induced phospholipidosis. This verification will aid in launching new avenues for further clinical application and management of DIPLosis.

Conclusion

Crocin has a protective effect against hepatic insult and DIPLosis, mediated by PI3K/Akt/mTOR signaling.

Abbreviations: *DIPLosis:* Drug induced phospholipidosis; *CAD:* cationic amphiphilic drugs; *TCAs:* tricyclic antidepressants; *AP1S1:* adaptor protein complexes 1 subunit 1; *ELOVL6:* Elongation of very long-chain fatty acids proteins 6; *SCD1:* Stearoyl-CoA desaturase 1; *HMGR:* 3-hydroxy-3-methylglutaryl-Coenzyme A reductase; *LPLA2:* lipoprotein-associated phospholipase A2; *mTORC1:* mechanistic Target of Rapamycin Complex 1; *PI3K:* Phosphoinositide 3 kinase; *TNF-α:* Tumor Necrosis Factor; *IL-6:* Interleukin 6; *TOS:* Total oxidant status; *TAC:* Total antioxidant capacity; *SOD:* super-oxide dismutase.

Funding: This research did not receive any specific grant from funding agencies in the public, commercial or not for profit sectors.

Data Availability: This published paper file includes all data created or assessed during this study.

Conflict of Interests: The authors declare the existence of all possible conflicts of interest, including financial, consultant, institutional and other relationships that might constitute a potential conflict of interest in relation to the subject matter of the article.

Author Contributions: All authors contributed to research formal analysis, methodology, writing original draft, reviewing, editing and statistical analysis. All authors critically revised the manuscript and gave final approval.

References

1. Kaplowitz N. Drug-induced liver injury. Clin Infect Dis 2004;38:S44–48. doi: 10.1086/381446.
2. Shahane SA, Huang R, Gerhold D, et al. Detection of phospholipidosis induction: a cell-based assay in high-throughput and high-content format. J Biomol Screen 2014;19:66–76. doi: 10.1177/1087057113502851.
3. Xia Z, Ying G, Hansson AL, et al. Antidepressant-induced lipidosis with special reference to tricyclic compounds. Prog Neurobiol 2000 Apr;60(6):501–12. doi: 10.1016/s0301-0082(99)00036-2.
4. Hicks JK, Swen JJ, Thorn CF, et al. Clinical Pharmacogenetics Implementation Consortium. Clinical Pharmacogenetics Implementation Consortium guideline for CYP2D6 and CYP2C19 genotypes and dosing of tricyclic antidepressants. Clin Pharmacol Ther 2013;93:402–408. doi: 10.1038/clpt.2013.2.
5. Vukotić NT, Đorđević J, Pejić S, et al. Antidepressants- and antipsychotics-induced hepatotoxicity. Arch Toxicol 2021 Mar;95(3):767-789. doi: 10.1007/s00204-020-02963-4.
6. Lucena, MI, Carvajal A, Andrade RJ, et al. Antidepressant-induced hepatotoxicity. Expert Opin Drug Saf 2003;2:249–262. doi: 10.1517/14740338.2.3.249.
7. Boehm M, Bonifacino JS. Adaptins. The final recount. Mol Biol Cell 2001;12:2907–2920. doi: 10.1091/mbc.12.10.2907.

8. Sorkin A. Cargo recognition during clathrin-mediated endocytosis: a team effort. Curr Opin Cell Biol 2004;16: 392–399. doi: 10.1016/j.ceb.2004.06.001.
9. Newell-Litwa K, Seong E, Burmeister M, et al. Neuronal and non-neuronal functions of the AP-3 sorting machinery. J Cell Sci 2007;120:531–541. doi: 10.1242/jcs.03365.
10. Peláez R, Pariente A, Pérez-Sala Á, et al. Sterculic acid: the mechanisms of action beyond stearoyl-coA desaturase inhibition and therapeutic opportunities in human diseases. Cells 2020;9:140. doi: 10.3390/cells9010140.
11. Corominas J, Ramayo-Caldas Y, Puig-Oliveras A, et al. Polymorphism in the ELOVL6 gene is associated with a major QTL effect on fatty acid composition in pigs. PLoS One 2013;8:e53687. doi: 10.1371/journal.pone.0053687.
12. Knebel B, Haas J, Hartwig S, et al. Liver-specific expression of transcriptionally active SREBP-1c is associated with fatty liver and increased visceral fat mass. PLoS One 2012;7:e31812. doi: 10.1371/journal.pone.0031812.
13. Matsuzaka T, Shimano H, Yahagi N, et al. Cloning and characterization of a mammalian fatty acyl-CoA elongase as a lipogenic enzyme regulated by SREBPs. J Lipid Res 2002;43:911–920. PMID: 12032166.
14. Thelen AM, Zoncu R. Emerging roles for the lysosome in lipid metabolism. Trends Cell Biol 2017;27:833–850. doi: 10.1016/j.tcb.2017.07.006.
15. Escribano J, Alonso GL, Coca-Prados M, et al. Crocin, safranal and picrocrocin from saffron (Crocus sativus L.) inhibit the growth of human cancer cells in vitro. Cancer Lett 1996;100,23–30. doi: 10.1016/0304-3835(95)04067-6.
16. Luo L, Fang K, Dan X, et al. Crocin ameliorates hepatic steatosis through activation of AMPK signaling in db/db mice. Lipids Health Dis 2019;18:11. doi: 10.1186/s12944-018-0955-6.
17. Razavi BM, Hosseinzadeh H, Abnous K, et al. Protective effect of crocin on diazinon induced vascular toxicity in subchronic exposure in rat aorta ex-vivo. Drug Chem Toxicol 2014;37:378–383. doi: 10.3109/01480545.2013.866139.
18. Kozisek ME, Deupree JD, Burke WJ, et al. Appropriate dosing regimens for treating juvenile rats with desipramine for neuropharmacological and behavioral studies. J Neurosci Methods 2007;163: 83–91. doi: 10.1016/j.jneumeth.2007.02.015.
19. Bradford MM. A rapid and sensitive method for the quantitation of microgram quantities of protein utilizing the principle of protein-dye binding. Anal Biochem 1976;72: 248–254. doi: 10.1006/abio.1976.9999.
20. Erel O. A new automated colorimetric method for measuring total oxidant status. Clin Biochem 2005;38:1103–1111. doi: 10.1016/j.clinbiochem.2005.08.008.
21. Erel O. A novel automated direct measurement method for total antioxidant capacity using a new generation, more stable ABTS radical cation. Clin Biochem 2004;37:277–285. doi: 10.1016/j.clinbiochem.2003.11.015.
22. Livak KJ, Schmittgen TD. Analysis of relative gene expression data using real-time quantitative PCR and the 2(-Delta Delta C(T)) Method. Methods 2001;25:402–408. doi: 10.1006/meth.2001.1262.
23. Kuo J. Electron Microscopy: Methods and Protocols. 2nd ed. Humana Press Inc.: Totowa, NJ, 2007.
24. Halliwell WH. Cationic amphiphilic drug-induced phospholipidosis. Toxicol Pathol 1997;25:53–60. doi: 10.1177/019262339702500111.
25. Breiden B, Sandhoff K. Emerging mechanisms of drug-induced phospholipidosis. Biol Chem 2019;401:31–46. doi: 10.1515/hsz-2019-0270. Erratum in: Biol Chem. 2021 Oct 27, 403(2), 251.
26. Schulze H, Kolter T, Sandhoff K. Principles of lysosomal membrane degradation: Cellular topology and biochemistry of lysosomal lipid degradation. Biochim Biophys Acta 2009;1793: 674–683. doi: 10.1016/j.bbamcr.2008.09.020.
27. Stäubli W, Schweizer W, Suter J. Some properties of myeloid bodies induced in rat liver by an antidepressant drug (maprotiline). Exp Mol Pathol 1978;28:177–195. doi: 10.1016/0014-4800(78)90050-3.
28. Bockhardt H, Lüllmann-Rauch R. Zimelidine-induced lipidosis in rats. Acta Pharmacol Toxicol 1980;47:45–48. doi: 10.1111/j.1600-0773.1980.tb02023.x.
29. Lüllmann-Rauch R, Nässberger L. Citalopram-induced generalized lipidosis in rats. Acta Pharmacol Toxicol 1983;52:161–167. doi: 10.1111/j.1600-0773.1983.tb01080.x.
30. Chen J, Bai L, He Y. A possible case of carbamazepine-induced renal phospholipidosis mimicking Fabry disease. Clin Exp Nephrol 2022;26:303–304. doi: 10.1007/s10157-021-02172-y.
31. Hinkovska-Galcheva, V, Treadwell T, Shillingford JM, et al. Inhibition of lysosomal phospholipase A2 predicts drug-induced phospholipidosis. J Lipid Res 2021;62:100089. doi: 10.1016/j.jlr.2021.100089.
32. Sawada H, Takami K, Asahi S. A toxicogenomic approach to drug-induced phospholipidosis: analysis of its induction mechanism and establishment of a novel in vitro screening system. Toxicol Sci 2005;83:282–292. doi: 10.1093/toxsci/kfh264.
33. Matsuzaka T, Kuba M, Koyasu S, et al. Hepatocyte ELOVL fatty acid elongase 6 determines ceramide acyl-chain length and hepatic insulin sensitivity in mice. Hepatology 2020;71:1609–1625. doi: 10.1002/hep.30953.
34. Matsuzaka T. Role of fatty acid elongase Elovl6 in the regulation of energy metabolism and pathophysiological significance in diabetes. Diabetol Int 2020;12:68–73. doi: 10.1007/s13340-020-00481-3.
35. Rodriguez-Cuenca S, Whyte L, Hagen R, et al. Stearoyl-CoA desaturase 1 is a key determinant of membrane lipid composition in 3t3-l1 adipocytes. PLoS One 2016;11: e0162047. doi: 10.1371/journal.pone.0162047.
36. Datta S, Wang L, Moore DD, et al. Regulation of 3-hydroxy-3-methylglutaryl coenzyme A reductase promoter by nuclear receptors liver receptor homologue-1 and small heterodimer partner: a mechanism for differential regulation of cholesterol synthesis and uptake. J Biol Chem 2006;281:807–812. doi: 10.1074/jbc.M511050200.
37. Wang T, Zhao Y, You Z, et al. Endoplasmic reticulum stress affects cholesterol homeostasis by inhibiting LXRα

expression in hepatocytes and macrophages. Nutrients 2020;12:3088. doi: 10.3390/nu12103088.
38. DeSanty KP, Amabile CM. Antidepressant-induced liver injury. Ann Pharmacother 2007;41:1201–12,11. doi: 10.1345/aph.1K114.
39. Voican CS, Corruble E, Naveau S, et al. Antidepressant-induced liver injury: a review for clinicians. Am J Psychiatry 2014;171:404–415. doi: 0.1176/appi.ajp.2013.13050709.
40. Ye H, Nelson LJ, Gómez Del Moral M, et al. Dissecting the molecular pathophysiology of drug-induced liver injury. World J Gastroenterol 2018;24:1373–1385. doi: 10.3748 /wjg.v24.i13.1373.
41. Ohkuma S, Poole B. Cytoplasmic vacuolation of mouse peritoneal macrophages and the uptake into lysosomes of weakly basic substances. J Cell Biol 1981;90:656–664. doi: 10.1083/jcb.90.3.656.
42. Morissette G, Moreau E, C-Gaudreault R, et al. Massive cell vacuolization induced by organic amines such as procainamide. J Pharmacol Exp Ther 2004;310:395–406. doi: 10.1124/jpet.104.066084.
43. Trump BF, Goldblatt PJ, Stowell RE. Studies of mouse liver necrosis in vitro. Ultrastructural and cytochemical alterations in hepatic parenchymal cell nuclei. Lab Invest 1965;14:1969–1999. PMID: 5854188.
44. Czaja MJ, Ding WX, Donohue TM, et al. Functions of autophagy in normal and diseased liver. Autophagy 2013;9: 1131–1158. doi: 10.4161/auto.25063.
45. Anderson N, Borlak J. Drug-induced phospholipidosis. FEBS Lett 2006;580:5533–5540. doi: 10.1016/j.febslet. 2006.08.061.
46. Arimochi H, Morita K. Desipramine induces apoptotic cell death through nonmitochondrial and mitochondrial pathways in different types of human colon carcinoma cells. Pharmacology 2008; 81:164–172. doi: 10.1159/000111144.
47. Ríos-Arrabal S, Artacho-Cordón F, León J. et al. Involvement of free radicals in breast cancer. Springerplus 2013; 2:404. doi: 10.1186/2193-1801-2-404.
48. Estaquier J, Vallette F, Vayssiere JL, et al. The mitochondrial pathways of apoptosis. Adv Exp Med Biol 2012;942: 157–183. doi: 10.1007/978-94-007-2869-1_7.
49. Yang DK, Kim SJ. Desipramine induces apoptosis in hepatocellular carcinoma cells. Oncol Rep. 2017;38:1029–1034. doi: 10.3892/or.2017.5723.
50. Huang YY, Peng CH, Yang YP, et al. Desipramine activated Bcl-2 expression and inhibited lipopolysaccharide-induced apoptosis in hippocampus-derived adult neural stem cells. J Pharmacol Sci 2007;104:61–72. doi: 10.1254/jphs. fp0061255.
51. Vejux A, Guyot S, Montange T, et al. Phospholipidosis and down-regulation of the PI3-K/PDK-1/Akt signalling pathway are vitamin E inhibitable events associated with 7-ketocholesterol-induced apoptosis. J Nutr Biochem 2009;20:45–61. doi: 10.1016/j.jnutbio.2007.12.001.
52. Feng FB, Qiu HY. Effects of Artesunate on chondrocyte proliferation, apoptosis and autophagy through the PI3K/Akt /mTOR signaling pathway in rat models with rheumatoid arthritis. Biomed Pharmacother 2018;102:1209–1220. doi: 10.1016/j.biopha.2018.03.142.
53. Assimopoulou AN, Sinakos Z, Papageorgiou VP. Radical scavenging activity of Crocus sativus L. extract and its bioactive constituents. Phytother Res 2005;19:997–1000. doi: 10.1002/ptr.1749.
54. Nam KN, Park YM, Jung HJ, et al. Anti-inflammatory effects of crocin and crocetin in rat brain microglial cells. Eur J Pharmacol 2010;648:110–116. doi: 10.1016/j.ejphar .2010.09.003.
55. Amin A, Bajbouj K, Koch A, et al. Defective autophagosome formation in p53-null colorectal cancer reinforces crocin-induced apoptosis. Int J Mol Sci 2015;16: 1544–1561. doi: 10.3390/ijms16011544.
56. Lee IA, Lee JH, Baek NI, et al. Antihyperlipidemic effect of crocin isolated from the fructus of Gardenia jasminoides and its metabolite Crocetin. Biol Pharm Bull 2005;28: 2106–2110. doi: 10.1248/bpb.28.2106.
57. Behrouz V, Dastkhosh A, Hedayati M, et al. The effect of crocin supplementation on glycemic control, insulin resistance and active AMPK levels in patients with type 2 diabetes: a pilot study. Diabetol Metab Syndr 2020;12:59. doi: 10.1186/s13098-020-00568-6.
58. El-Beshbishy HA, Hassan MH, Aly HA, et al. Crocin "saffron" protects against beryllium chloride toxicity in rats through diminution of oxidative stress and enhancing gene expression of antioxidant enzymes. Ecotoxicol Environ Saf 2012;83:47–54. doi: 10.1016/j.ecoenv.2012.06.003.
59. Mozaffari S, Ramezany Yasuj S, Motaghinejad M, et al. Crocin acting as a neuroprotective agent against methamphetamine-induced neurodegeneration via CREB-BDNF signaling pathway. Iran J Pharm Res 2019;18:745–758. doi: 10.22037/ijpr.2019.2393.
60. Salahshoor MR, Khashiadeh M, Roshankhah S, et al. Protective effect of crocin on liver toxicity induced by morphine. Res Pharm Sci 2016(11):120–129.
61. Pilichos C, Preza A, Kounavis I, et al. Fine structural alterations induced by cortisol administration in non-adrenalectomized/non-fasted rat hepatocytes. Int Immunopharmacol 2005;5:93–96. doi: 10.1016/j.intimp.2004.09.004.
62. Razavi BM, Hosseinzadeh H, Movassaghi AR, et al. Protective effect of crocin on diazinon induced cardiotoxicity in rats in subchronic exposure. Chem Biol Interact 2013;203:547–555. doi: 10.1016/j.cbi.2013.03.010.
63. Mehri S, Abnous K, Mousavi SH, et al. Neuroprotective effect of crocin on acrylamide-induced cytotoxicity in PC12 cells. Cell Mol Neurobiol 2012;32:227–235. doi: 10.1007 /s10571-011-9752-8.
64. Hosseinzadeh H, Shamsaie F, Mehri S. Antioxidant activity of aqueous and ethanolic extracts of Crocus sativus L. stigma and its bioactive constituents, crocin and safranal. Pharmacogn Mag 2009;5:419–424. Corpus ID: 94582248.
65. Xu GL, Yu SQ, Gong ZN, et al. Study of the effect of crocin on rat experimental hyperlipemia and the underlying mechanisms. Zhongguo Zhong Yao Za Zhi 2005;30:369–372. Chinese. PMID: 15806972.

66. Vahdati Hassani F, Mehri S, Abnous K, et al. Protective effect of crocin on BPA-induced liver toxicity in rats through inhibition of oxidative stress and downregulation of MAPK and MAPKAP signaling pathway and miRNA-122 expression. Food Chem Toxicol 2017;107:395–405. doi: 10.1016/j.fct.2017.07.007.
67. Kim EK, Choi EJ. Compromised MAPK signaling in human diseases: an update. Arch Toxicol 2015;89:867–882. doi: 10.1007/s00204-015-1472-2.
68. Esau C, Davis S, Murray SF, et al. MiR-122 regulation of lipid metabolism revealed by in vivo antisense targeting. Cell Metab 2006;3:87–98. doi: 10.1016/j.cmet.2006.01.005.
69. Li K, Li Y, Ma Z, et al. Crocin exerts anti-inflammatory and anti-catabolic effects on rat intervertebral discs by suppressing the activation of JNK. Int J Mol Med. 2015 Nov;36(5):1291-9. DOI: 10.3892/ijmm.2015.2359
70. Qi Y, Chen L, Zhang L, et al. Crocin prevents retinal ischaemia/reperfusion injury-induced apoptosis in retinal ganglion cells through the PI3K/Akt signalling pathway. Exp Eye Res 2013;107:44–51. doi: 10.1016/j.exer.2012.11.011.
71. Salama RM, Abdel-Latif GA, Abbas SS, et al. Neuroprotective effect of crocin against rotenone-induced Parkinson's disease in rats: Interplay between PI3K/Akt signaling pathway and enhanced expression of miRNA-7 and miRNA-221. Neuropharmacology 2020;164:107900. doi: 10.1016/j.neuropharm.2019.107900.

Correspondence:
Received: 27 February 2023
Accepted: 27 March 2023
Dr. Rowida Raafat Ibrahim, PhD
Assistant Professor of Medical Biochemistry & Molecular Biology Department, Faculty of Medicine, Tanta University, El-Geesh St, Tanta, Egypt. postal code: 31511
Telephone: 01117076606
E-mail: rowaida.yousef@med.tanta.edu.eg,
E-mail: dody2008too@windowslive.com
ORCID ID: 0000-0002-6500-8156